Chemistry & Biology, Vol. 11, 939–948, July, 2004, ©2004 Elsevier Ltd. All rights reserved. DOI 10.1016/j.chembiol.2004.04.013

A Distance Ruler for RNA Using EPR and Site-Directed Spin Labeling

Nak-Kyoon Kim, Ayaluru Murali, and Victoria J. DeRose*
Department of Chemistry
Texas A&M University
College Station, Texas 77842

Summary

As a basic model study for measuring distances in RNA molecules using continuous wave (CW) EPR spectroscopy, site-directed spin-labeled 10-mer RNA duplexes and HIV-1 TAR RNA motifs with various interspin distances were examined. The spin labels were attached to the 2′-NH_2 positions of appropriately placed uridines in the duplexes, and interspin distances were measured from both molecular dynamics simulations (MD) and Fourier deconvolution methods (FD) [13]. The 10-mer duplexes have interspin distances ranging from 10 Å to 30 Å based on MD; however, dipolar line broadening of the CW EPR spectrum is only observed for the RNAs for predicted interspin distances of 10–21 Å and not for distances over 25 Å. The conformational changes in TAR (transactivating responsive region) RNA in the presence and in the absence of different divalent metal ions were monitored by measuring distances between two nucleotides in the bulge region. The predicted interspin distances obtained from the FD method and those from MD calculations match well for both the model RNA duplexes and the structural changes predicted for TAR RNA. These results demonstrate that distance measurement using EPR spectroscopy is a potentially powerful method to help predict the structures of RNA molecules.

Introduction

Distance measurements between two site-specific probes in biomolecules are a powerful method to determine or constrain structures, particularly for large or dynamically complex systems. For proteins, site-directed spin labeling (SDSL) in conjunction with EPR spectroscopy has been used broadly for this purpose [1–5]. SDSL has not been broadly applied to RNA structural biology, despite a constant need for additional tools to predict RNA folding and RNA-protein complex formation. The goal of this work is to develop SDSL for distance measurements in RNA complexes.

SDSL introduces spin-label molecules into desired positions of macromolecules. In the case of proteins, thiol-reactive nitroxide spin labels have been introduced mainly to cysteine-substituted sites [2–5]. For RNA oligonucleotides, spin labels can be covalently attached either to modified bases [6–8] or the phosphate moiety [9, 10], or to the 2′ position of the ribose ring [11, 12]. Spin-label attachment to the bases of oligonucleotides is useful for loop or bulge regions where the bases are not involved in Watson-Crick hydrogen bonding, or 3′ or 5′ ends where base pairing will not significantly affect the oligonucleotide tertiary structures. A 2′ modification for the spin-labeling sites may be advantageous for SDSL, because this modification may not be restricted to the sequence of the oligonucleotides, and it may have lesser consequences for base pairing [12].

SDSL in conjunction with EPR spectroscopy has been used to measure distances in protein systems through measuring spin-spin dipolar couplings. For example, the distances between nitroxides attached to synthetic α-helical polypeptides have been predicted with a range of inter-spin distances from 8 to 25 Å using Fourier deconvolution of the EPR spectra [13]. Various EPR methods, including monitoring the half-field transition, Fourier deconvolution, computer simulation of line shapes, and pulsed EPR techniques, have been compared for distance measurements in proteins (reviewed in [14]). Although actual distances were not measured from the EPR spectra, the interactions between protein and RNA in ribonuclease P from *Escherichia coli* were monitored by the dynamics of the spin-label molecules attached to several cysteine residues in the protein [15]. Recently, a 60 Å distance in a short RNA oligonucleotide labeled via internal 2′-NH_2 positions was measured using pulsed electron double resonance (PELDOR) spectroscopy [16]. However, there are no studies in the literature reporting a range of distance measurements in RNA molecules using more commonly available continuous wave (CW) EPR spectroscopy.

Functional RNAs such as ribozymes have compact and highly folded tertiary structures, and the correct folding is critical to the activity of these molecules [17]. For example, based on FRET studies, the hammerhead ribozyme has been proposed to undergo a two-step folding pathway to form a catalytically active structure that is dependent on metal ion concentrations [18]. Recently, the folding and catalysis of the hairpin ribozyme has also been investigated with single molecule fluorescence methods [19, 20]. SDSL with EPR spectroscopy is a complementary method that may have certain merits; nitroxide spin labels are usually smaller than fluorophore molecules, and only one type of spin label is required for the two labeling sites. Interpretation of FRET can sometimes be complicated due to incomplete averaging of the relative orientation of the fluorophores, whereas the anisotropy of the nitroxide spin label is more easily approximated [21, 1].

As a model study for measuring distances within RNA molecules, and in order to apply this method to predict the folding pathways of larger RNA molecules, six different short 10-mer RNA duplexes have been designed with spin labels attached at varying 2′ positions (Figure 1) such that the interspin distances vary between ~9–30 Å. (Figure 2A). The thermodynamic consequence of label attachment on duplex stability was determined. The low-temperature EPR spectra of the doubly labeled

*Correspondence: derose@mail.chem.tamu.edu

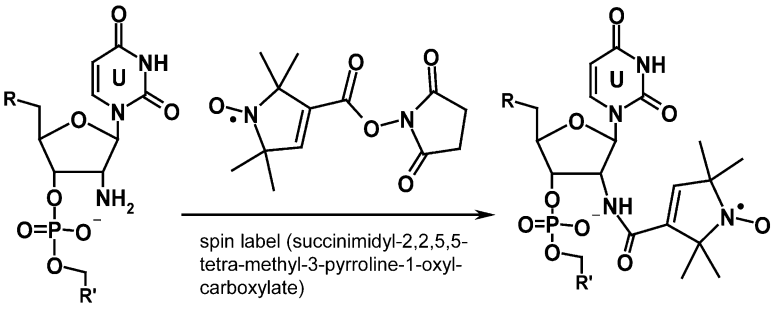

Figure 1. Spin-Labeling Reaction for 2′-NH_2 Modified RNA Oligonucleotides

duplexes showed spin-spin dipolar line broadening for distances ≤25Å, and these signals were analyzed by the Fourier deconvolution method [13]. Molecular modeling was performed for all duplexes to compare theoretical distances with experimental values.

Expanding from simple duplex models, SDSL was also used to observe structural changes predicted for an HIV-1 TAR RNA structure upon addition of divalent metal ions. The HIV Tat protein binds to TAR RNA around the trinucleotide bulge region to activate HIV gene expression (Figure 3A) [22, 23]. Biochemical and biophysical studies on a stem-loop TAR sequence have revealed that it undergoes structural changes upon binding to derivatives of Tat protein or metal ions [24–27]. In the absence of divalent metals, the upper and lower helical stems of the TAR RNA are predicted to fluctuate about an average bend angle of ~50° [24, 25, 27, 28]. Structural studies of TAR in the presence of 4.5 mM Mg^{2+}, 50 mM Ca^{2+} and 2.5 mM Mg^{2+}, or Tat peptide predict that the two helices are almost coaxially stacked (Figure 3A). In this work, conformational changes of TAR RNA upon binding divalent metal ions were examined by measuring distances between two attached spin labels. The data predict an increase in interspin distance in the presence of metal ions, consistent with expectations from molecular modeling. This study demonstrates that, with a straightforward protocol of SDSL and CW EPR spectroscopy, reliable distance measurements can be available for RNA systems.

Results

Design of the RNA Duplex Structures

Six RNA duplexes with 10 base pairs were designed to measure distances between attached nitroxide spin labels (Table 1). To increase the stability of each duplex, two G:C base pairs close the duplexes at both 3′ and 5′ ends. 2′-Modified uridines, to which spin labels were attached (Figure 1), were placed in the interior of the sequence to minimize adverse effects on the stability of the duplexes. As shown in Table 1, moving the position of a 2′-amino U in the sequence changes the predicted interspin distances. In order to be able to compare the EPR spectra of duplexes with either single or double spin labels, self-complementary sequences were not used.

Thermal Stability of the Spin-Labeled RNA Duplexes

In order to investigate the thermodynamic effects of the 2′ modifications, UV-Vis detected thermal denaturation experiments were performed for several modified duplexes (Table 2A). In 0.1 M NaCl (pH 7.8), the melting temperatures of the RNA duplexes without modification were approximately 56°C. A single 2′-amino modification on one nucleotide of a duplex destabilized the RNA structure by 2°C–3°C. When two 2′-amino groups were introduced, the duplex was destabilized by an additional 2°C–3°C. Upon attachment of the spin label to RNA duplexes, each labeling of a single strand destabilized the resulting duplex by approximately 10°C compared to the unmodified duplex.

Modeling of the Duplexes

Distances between nitrogen atoms of the two nitroxide spin labels were predicted using molecular modeling (Table 3A). The structures of the spin-labeled duplexes with averaged distances are shown in Figure 2A. While rotating the two spin labels in the simulation, the distributions of the spin-spin distances were obtained, and the ranges and average distances are listed in Table 3. Although the U7A/U5 duplex has the shortest interspin distance, averaged at 9.7 Å, and the spin label has a length including linker of 5–6 Å, the two spin labels did not inhibit the rotation of each other in this duplex.

Low-Temperature EPR Spectra

The EPR spectra for all duplexes were measured at low temperature (183K) to obtain the pure dipolar line broadening contribution to the EPR spectra. When the samples are frozen so that rotational and translational motions are restricted, the EPR spectra of these samples are the superposition of the spectrum of each spin with a different orientation in the external magnetic field, and the spectra can be treated as a powder pattern.

The EPR spectra of the doubly labeled duplexes show marked differences as the nitroxide interspin distance changes (Figure 2B). The spin-spin dipolar interaction leads to line broadening, which is observed as a decrease in intensity of the EPR spectra (red lines) relative to the additive spectra of two singly labeled samples (black lines). The dipolar interaction is not obvious in the CW EPR spectra of the U7/U8 and U8A/U8B duplexes, which have predicted interspin distances of ≥25 Å that exceed the detection limit using CW EPR spectroscopy.

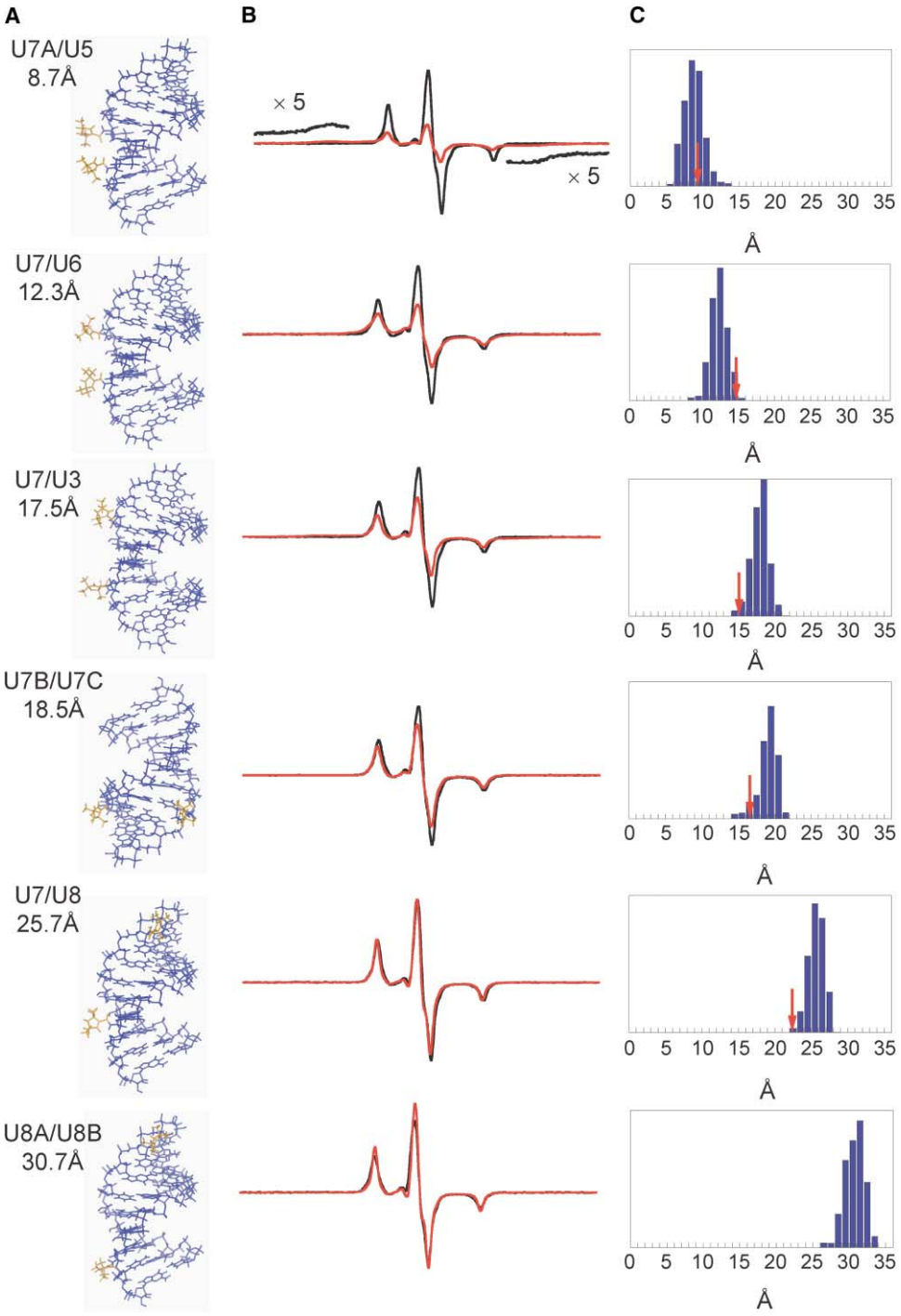

Figure 2. EPR Spectra and Predicted Interspin Distances for Spin-Labeled RNA Duplexes

(A) The structures of spin-labeled RNA 10-mers simulated within the *Discover 3* module in *Insight II*, assuming that the 10-mers have canonical rigid A-type RNA structures.

(B) EPR spectra of the doubly labeled 10-mer duplexes at 183K in 100 mM NaCl, 20% ethylene glycol, and 5 mM TEA buffer (pH 7.8). The summed spectra of two singly labeled duplexes are shown in black, and the spectra of doubly labeled duplexes are shown in red. Dipolar line broadening results in an apparent signal decrease for the doubly labeled duplexes.

(C) Distributions of the interspin distances for all duplexes predicted from MD calculations (blue) and the averaged interspin distances obtained from FD analysis of EPR spectra (red arrow).

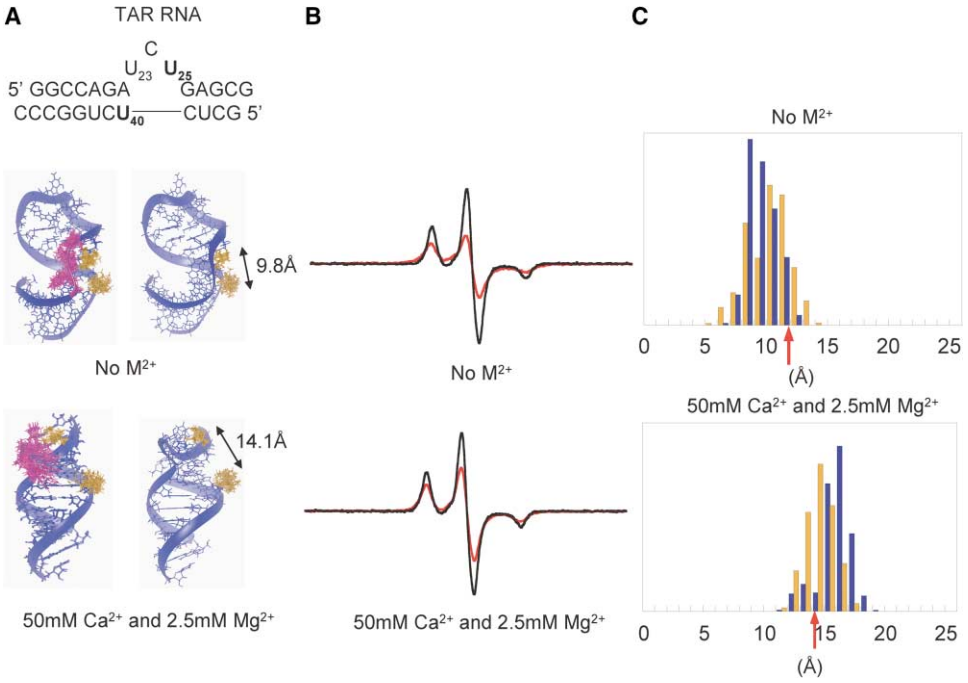

Figure 3. EPR Spectra and Predicted Interspin Distances for Spin-Labeled HIV-1 TAR RNA

(A) The secondary structure of TAR RNA and the tertiary structures of the spin labeled models used to predict distances under different metal ion conditions. Spin labels are attached to U25 and U40 (bold). In model structures, spin labels are highlighted in orange and the flexible bulge is colored in magenta.

(B) EPR spectra of the doubly labeled TAR RNA under different metal conditions (100K). Buffer contains 50 mM NaCl, 20% ethylene glycol, and 5 mM TEA buffer (pH 7.8). The summed spectra of two singly labeled duplexes are shown in black, and the spectra of doubly labeled duplexes are shown in red.

(C) Distributions of the interspin distances for TAR RNA predicted from MD calculations (orange for fixed RNA, blue for flexible bulge) and averaged interspin distances obtained from FD analysis of EPR spectra (red arrow).

However, the rest of the duplexes exhibit dipolar broadenings that increase as the estimated distances get smaller. Furthermore, the EPR spectrum of U7A/U5 shows additional shoulders at both lower and higher magnetic fields, which can be observed due to the exchange interaction between overlapping nitrogen π-orbitals of the nitroxide groups when the interspin distances are less than 1.0 nm [30, 31].

Fourier Deconvolution of the EPR Spectra

Dipolar line broadening functions for all duplexes were obtained using Fourier deconvolution, and the averaged spin-spin distances were calculated as described in Experimental Procedures. Table 3A and Figure 4 compare the distances obtained from molecular modeling with those from the Fourier deconvolution method, which are in good agreement within 1–3 Å. The Fourier deconvolution method is sufficiently sensitive to model the $\sim$25 Å interspin distance predicted for U7/U8, even though the weak dipolar broadening for this sample is barely visible in the EPR spectra (Figure 2B). The calculated distance from molecular modeling for the U8A/U8B 10-mer is $\sim$30 Å, and the Fourier deconvolution method does not result in a detectable broadening function for this distance.

Spin Labeling and Thermal Stability of TAR RNA

The sequence of TAR RNA tested in this study contains the helix-bulge-helix region known to bind Tat peptide derivatives. As described above, studies on the stem-

Table 1. RNA Sequences and Estimated Distances Used in This Study

Name	10-mer Sequences[a]	Distance (Å)[b]
U5	5′-C C U A U G G U G G-3′	9.7
U7A	3′-G G A U A C C A C C-5′	
U6	5′-C C U A G U G U G G-3′	12.1
U7	3′-G G A U C A C A C C-5′	
U3	5′-C C U A G U G U G G-3′	17.3
U7	3′-G G A U C A C A C C-5′	
U7B	5′-C C U A G G U U G G-3′	18.2
U7C	3′-G G A U C C A A C C-5′	
U8	5′-C C U A G U G U G G -3′	25.3
U7	3′-G G A U C A C A C C-5′	
U8A	5′-C G A U G U G U G C-3′	30.0
U8B	3′-G C U A C A C A C G-5′	
TAR15	5′-G G C C A G A U C U G A G C G-3′	9.8[c] (14.1)[d]
TAR12	3′-C C C G G U C U C U C G-5′	

[a] U indicates the 2′-NH_2 uridine where the spin label molecule is attached.

[b] Averaged distances based on MD calculations (see Table 3).

[c] Based on the NMR structure (PDB ID code 1ANR, structure 1).

[d] Based on the X-ray crystal structure (NDB ID code URX075).

Table 2. Thermal Stabilities of RNA Duplexes Used in This Study

A. Thermal Stabilities of the 2′-Modified RNA 10-mer Duplexes

Modification	$T_{m,\,average}$ (°C)
none	55.4 ± 0.5
single 2′-NH_2	52.3 ± 0.6
double 2′-NH_2	48.3 ± 0.6
single 2′- spin label	46.1 ± 0.8
double 2′- spin label	36.1 ± 1.5

B. Metal Dependence of the Thermal Stabilities of the TAR RNAs

	T_m (°C)			
[M^{2+}]	No Modification	L12/15	12/L15	L12/L15
no Mg^{2+}	52.0	50.2	50.2	47.0
50 mM Ca^{2+}, 2.5 mM Mg^{2+}	68.3	65.4	66.5	60.0

Melting temperatures were measured with UV-VIS spectroscopy in 5 mM TEA buffer (pH 7.8) and 100 mM NaCl for 10-mer duplexes and 50 mM NaCl (pH 7.8) for TAR RNAs. L stands for the labeled RNA.

Table 3. Spin-Spin Distances Determined from Molecular Dynamics and EPR Spectra Using the Fourier Deconvolution Method

A. Doubly Labeled 10-mer Duplexes

	d_{MD} (Å)		
RNA	Range	Average	$d_{FD,\,av}$ (Å)
U7A/U5	5.7–13.7	8.7	9.1 ± 0.3
U7/U6	8.5–15.6	12.3	14.8 ± 0.5
U7/U3	13.6–20.5	17.5	15.0 ± 0.5
U7B/U7C	13.8–21.2	18.5	16.5 ± 0.5
U7/U8	22.5–28.0	25.7	22.1 ± 0.7
U8A/U8B	25.9–34.0	30.7	NA

B. TAR RNA

	d_{MD} (Å)		
[M^{2+}]	Range	Average	$d_{FD,\,av}$ (Å)
None	5.1–13.8 (6.3–12.9)[a]	9.8 (9.1)	11.9 ± 0.3
50 mM Ca^{2+}, 2.5 mM Mg^{2+}	11.3–17.0 (11.2–19.0)	14.1 (15.5)	14.2 ± 0.3

[a] Distances in parentheses are calculated without structure constraints on the bulge nucleotides.

loop TAR containing this sequence predict that the RNA undergoes global and local structural changes depending on the type and concentrations of divalent metals. Two sites, U25 and U40, were chosen for spin labeling of TAR RNA such that the resulting interspin distances were modeled to be ≤25 Å (vide infra), and changes in them would report upon the predicted metal-dependant transition to coaxially stacked helices. These sites are in the bulge region of TAR and have previously been shown through SDSL to exhibit dynamic properties, as expected from solution NMR studies [11]. Attachment of spin labels at these sites has only a minor effect on melting temperature, decreasing T_m by only 2°C in the singly labeled and 5°C–8°C in doubly labeled TAR RNAs (Table 2).

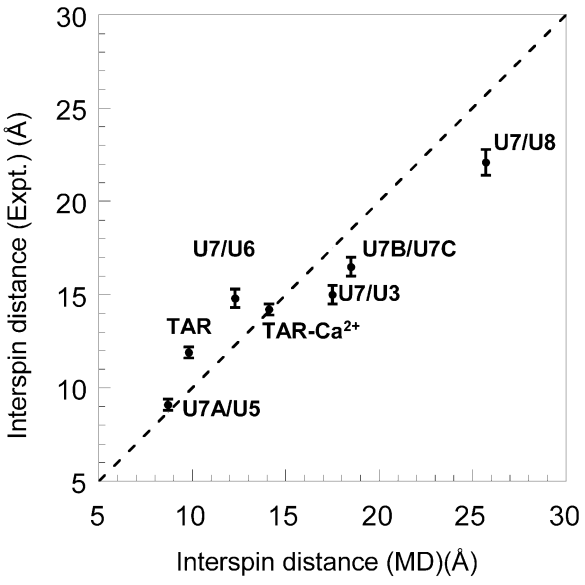

Figure 4. Comparison of Distances Measured from Fourier Deconvolution Analysis of EPR Spectra and from Computer Simulations with *Insight II*

TAR indicates TAR RNA without divalent metal, and TAR-Ca^{2+} indicates TAR RNA in the presence of 50 mM Ca^{2+} and 2.5 mM Mg^{2+}. Dashed line indicates the ideal correlation between experimental and MD values.

Modeling TAR RNA

In the absence of divalent cations, TAR is predicted to undergo significant conformational fluctuations [27, 28]. As an initial model for TAR RNA in the absence of divalent ions, one structure was chosen from a family of 20 conformers that satisfied NMR constraints obtained in ~50 mM NaCl at pH 5.5 (Protein Data Bank ID code 1ANR, structure 1) [25]. For estimating distance changes predicted for TAR in the presence of Ca^{2+}, the X-ray structure obtained from crystals grown in ~40 mM NaCl, 50 mM $CaCl_2$, and 2.5 mM $MgCl_2$ (pH 6.0) was used (NBD URX075) [26]. Since the nucleotides in the bulge region of the TAR RNA are considered to be flexible, simulations of spin-labeled TAR were performed in which those regions were either kept rigid or allowed to move relative to the helical regions. Based on these simulations, average interspin distances of 9.1–9.8 Å were predicted for labels attached to U25 and U40 of TAR in the absence of divalent metal ions. These distances were predicted to increase to 14.1–15.5 Å upon addition of divalent ions (Table 3B).

EPR Distance Measurements in TAR RNA

As described by Edwards and Sigurdsson [11], the room temperature EPR spectra of individual spin labels at U25 and U40 show differences in line shapes (data not shown) that reflect increased mobility for U25. The line shapes of the doubly labeled TAR RNA EPR spectra, obtained at 100K (Figure 3B), are further broadened due

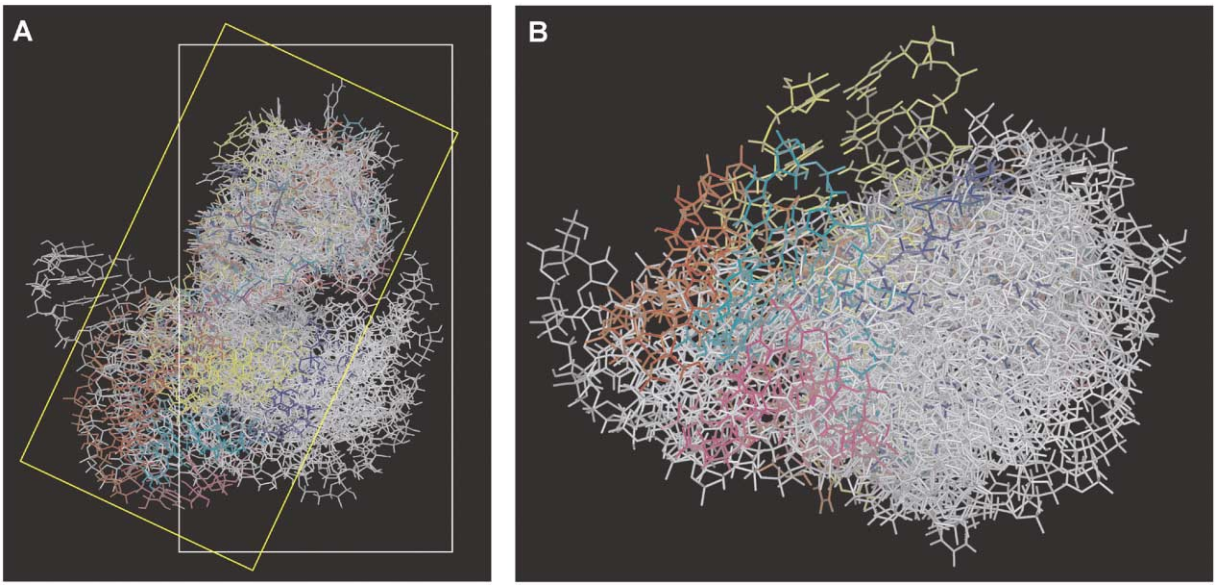

Figure 5. Overlay of Predicted TAR RNA Structures

A side view (A) and a bottom view (B) of the overlaid 20 conformers of TAR RNA retrieved from Protein Data Bank ID code 1ANR. Five structures that have interspin distances predicted to be within ±3 Å about the EPR-measured value are highlighted (yellow box), and the remaining structures are in white (white box).

to dipolar interactions, as expected. Metal-dependent EPR spectra of doubly spin-labeled TAR RNA obtained at 100K are shown in Figure 3B. The amount of broadening is similar to that observed for the U7U6 and U7U3 model duplexes, indicating that similar interspin distances in the region of 12–15 Å are expected. Moreover, a lower apparent intensity is observed in the case of TAR without divalent cations, indicating that the interspin distance is shorter than that observed upon addition of Ca^{2+}. Indeed, the distances obtained from the Fourier deconvolution methods are 11.9 ± 0.3 Å for TAR RNA in the absence of divalent cations (0.1 M NaCl) and 14.2 ± 0.3 Å when 50 mM Ca^{2+} is added. These distances are similar to those predicted by molecular modeling, and the change observed is consistent with the increase in distance between the nitroxide spin labels that is predicted upon coaxial stacking of the TAR RNA helices upon binding of divalent cations.

Restricting TAR RNA Structural Models by EPR Distance Measurements

In theory, the interspin distance of 11.9 ± 0.3 Å measured for TAR RNA in 0.1 M NaCl can be used as an additional constraint in calculating structures based on solution NMR data. As an initial demonstration, the 20 structures published for TAR were evaluated in order to determine whether a subset of them would fit the SDSL data. Following MD simulations for all 20 structures modeled with added spin labels at U25 and U40, only five structures were found to have interspin distances within a broad range of ±3 Å about the experimentally determined value. Figure 5 shows an overlay of all 20 TAR RNA conformers in which the five selected structures are distinguished in colors, and the remaining structures are in white. It is apparent that the selected structures sample a subset of interhelical orientations.

Discussion

Measuring distances between localized labels is an important method for obtaining structural information about biological macromolecules. While EPR methods have been used widely to probe structure and dynamics in proteins, these have been far less explored for complex RNA molecules. In this study, A-type RNA 10-mer duplexes with different interspin distances were tested as a basic model for measuring distances in RNA molecules using site-directed spin labeling with EPR spectroscopy. In addition, the conformational changes of a helix-bulge-helix motif of TAR RNA were examined as a function of different ionic conditions.

One challenge in using SDSL for RNA studies is attachment of the label. Recently, 2′-amino modifications have been successfully employed for attaching probes in RNA molecules. This method provides a convenient tool for introducing labels to the ribose ring at any position in the RNA sequence. For example, a ribose 2′-amino modification has been used to attach pyrene fluorophores internally to the P4-P6 domain of the *Tetrahymena* group I intron in order to monitor the tertiary folding [32]. More recently, Edwards and Sigurdsson attached an isocyanate nitroxide spin label to the 2′ amino of a uridine to study dynamics in TAR RNA using EPR spectroscopy [11]. Here, we used 2′-amino modified uridine to introduce a commercially available n-succinimidyl spin label internally to RNA sequences.

A decrease in thermal stabilities of the 10-mer du-

plexes is observed for RNAs containing 2′-amino modifications. An additive decrease in the thermal melting temperature of duplexes upon ribose 2′-NH_2 modification was previously observed in the thermal stabilities of 2′-amino modified 9-mer RNA duplexes [33]. There, 2′-amino modification in a single strand of a duplex caused destabilization of the RNA duplex by approximately 4°C, and three 2′-amino groups in consecutive cytidines of a single strand in an RNA duplex decreased the melting temperature by ~13°C. It has been proposed that 2′-amino modification destabilizes A-type RNA duplexes because the modification stabilizes a 2′-endo sugar pucker (~80%), as opposed to the otherwise dominant 3′-endo conformation [34]. Additional modification at the 2′ position with the spin label used here, which creates a relatively rigid amide linker, causes further destabilization but does not interfere with helix formation at room temperature or below. This level of destabilization may be less significant in the context of longer RNA helices, certain RNA tertiary structures, or with different linker lengths. Consistent with this, spin labels at the bulge region of TAR RNA have much less of an effect on the RNA stabilities (Table 2B; [11]). These results suggest that spin labels attached to nucleotides that are not involved in base stacking or are at the end of stacked regions may not significantly destabilize the RNA structures.

The interspin distances for the spin-labeled 10-mer duplexes investigated here were modeled based on the assumption that the RNA structure was rigid and was not affected by the different conformations of the spin labels that were sampled during the MD simulations. Figure 2C shows the distributions of interspin distances calculated from MD simulations in comparison with the averaged distances obtained from FD analysis of the EPR spectra. Averaged distances are also compared in Table 3A and Figure 4. The agreement between measured and predicted spin-spin distances indicates that the approximations used for MD simulation of the interspin distances are reasonable, despite the possibility that the sugar pucker may be altered at the labeled site.

Based on success with the model duplexes, we applied SDSL to monitor conformational changes in the more complex structure of TAR RNA. As predicted from MD calculations on models of TAR with conjugated spin labels, the distances between spin labels for TAR RNA are found to increase with addition of Ca^{2+}. This result is consistent with proposals that the helices become coaxially stacked upon addition of Ca^{2+}. For TAR in the absence of divalent ions, several studies have predicted conformational flexibility in the bulge region, which may lead to a distribution of angles between the helices. The average measured distance of ~12 Å between spin labels attached to U25 and U40 reflects the *majority* of the population as captured in a frozen solution. This value can help constrain the lowest-energy populations of TAR structures, as shown in Figure 5, but does not rule out the possibility that multiple structures with similar interspin distances are sampled due to dynamic flexibility. Addition of a second interspin distance constraint would narrow down the choice of conformers. Recently, dipolar broadening data have also been fit by a weighted sum of Pake functions [35, 36]. A preliminary distribution analysis for TAR suggests some populations with longer interspin distances (data not shown), consistent with predictions that conformers closer to the "stacked" collinear structures are also sampled [27–29].

The data in Figure 4 summarize the distances predicted from molecular dynamics simulations and SDSL experiments. Although there are 1–3 Å deviations from the linear dashed line that represents an ideal correlation, this method works quite well for estimating distances within 25 Å. The fitting procedure used here, with a single interspin distance, was chosen for simplicity. While the deviations increase the uncertainty in absolute distances to ±2 Å, the method used here will suffice for deducing large structural changes and also *relative* changes in distances caused by, for example, a shift in helix register. As demonstrated for TAR RNA, the method used here could also provide additional constraints in modeling solution NMR data, possibly to augment residual dipolar coupling calculation used to predict angles between RNA helices [37]. It should be noted that although distance determinations using this CW EPR spectroscopy/Fourier deconvolution method are limited to ranges of 8–25 Å [1], advanced EPR techniques such as pulsed electron double resonance (PELDOR) can be used, with the identical spin-labeling protocol, for the longer distance range of 20 Å to ~60 Å [16] (N.-K.K., V.J.D., and M.K. Bowman, unpublished results).

Significance

Although many studies measuring distances in protein systems have been successfully performed using continuous wave EPR spectroscopy, this technique has not been reported for RNA structures. In this study, we advanced the spectroscopic distance ruler previously reported for polypeptides to a model RNA duplex system for the first time and applied this method to TAR RNA for predicting conformational changes. Thus, distances between two spin labels attached to specific positions were measured using CW EPR spectroscopy and evaluated using Fourier deconvolution of the resulting dipolar-broadened line shapes. The results match well with interspin distances predicted from molecular simulations. This method will allow determination of inter- or intramolecular RNA interactions upon folding of RNA or protein binding and may add distance constraints for structures of RNA obtained from NMR experiments.

Experimental Procedures

RNA Oligonucleotides

All RNA 10-mer oligonucleotides were purchased from Dharmacon Research, Inc. (Lafayette, CO) and deprotected according to the vendor's instructions. The RNA sequences are listed in Table 1, where the symbol U in the name of the sequence stands for the 2′-NH_2 containing uridine nucleotide, and the numbers in 10-mer indicate the position of this uridine from the 5′ end. Deprotected RNAs that were not used for spin labeling were purified by 20% denaturing PAGE, dialyzed with 5 mM triethanolamine (TEA) and 100 mM NaCl buffer (pH 7.8) for 2 days at 4°C, and ethanol precipitated

overnight. The RNA pellets were dried and redissolved in 5 mM TEA and 100 mM NaCl buffer (pH 7.8) and stored at −30°C for further use.

Spin Labeling of RNA 10-mers

The spin label (succinimidyl-2,2,5,5-tetramethyl-3-pyrroline-1-oxyl-carboxylate) was obtained from ACROS (Fisher Scientific), and directly used for RNA labeling without further purification. The spin labels were attached to the RNA oligonucleotide 2′-NH_2 positions by a simple one-step reaction (Figure 1). In a typical reaction, 100 μl of 200 mM spin label in DMF was added to 100 μl of ~1 mM RNA in 0.5 M sodium phosphate and 0.5 mM EDTA buffer (pH 8.0). The reaction mixture was constantly stirred for 8 hr at 60°C, and then the RNA was precipitated in 3× volume of ethanol. The RNA pellet was resuspended in 400 μl of water and purified by 20% denaturing PAGE, electro-eluted from the gel, and concentrated via centrifugation (Centricon YM-3, Millipore). In order to separate labeled RNA from unreacted RNA, reverse-phase HPLC was performed with a C-18 column, 50 mM triethylammonium acetate (aqueous buffer A [pH 7.0]) and a mixture of 30% (v/v) buffer A with 70% (v/v) acetonitrile (organic buffer B) and 11%–23% gradient of buffer B. The spin-labeled RNA oligonucleotides were collected, dried by Speed Vac, resuspended in 5 mM TEA and 100 mM NaCl buffer (pH 7.8), transferred to Eppendorf tubes, and stored at −30°C.

The labeling efficiency of this method, which uses a commercially available nitroxide, is less than 50% for both 10-mer and TAR RNA sequences. The yield reduced to ~20% for a longer 35-mer RNA (our unpublished results), and this might be improved with addition of a denaturant to disrupt the RNA structure. Edwards and Sigurdsson have achieved >90% reported yield in labeling a 2′-NH_2 with an isocyanate derivative of tetramethylpiperidyl-*N*-oxy (TEMPO) nitroxide, synthesized by their published procedure [12].

Thermal Denaturation Experiments

The thermal melting profiles for both 10-mer duplexes and TAR RNA were obtained by monitoring at 260 nm and 280 nm on a CARY 300 Bio UV-VIS spectrometer (Varian). For 10-mers, 900 μl of 2 μM each of the complementary oligonucleotides in 5 mM TEA and 100 mM NaCl buffer (pH 7.8) were annealed at 90°C for 90 s and cooled for 30 min on ice to form duplexes. For TAR RNA, various metals were added after renaturation, and the final condition was 200 μl of 5 μM RNA hybrids in 5 mM TEA and 50 mM NaCl buffer (pH 7.8). Cuvettes (1 cm for 10-mers, 0.2 cm for TAR RNAs) were heated from 5°C to 95°C or 100°C at a rate of 0.3°C/min, and the first derivatives were calculated to obtain melting temperatures.

EPR Measurements with Spin-Labeled RNA Duplexes

EPR measurements were carried out in a Bruker EMX X-band spectrometer. Fifty microliters of 150 μM spin-labeled RNA duplexes in 5 mM TEA, 20%(v/v) ethylene glycol, and 100 mM NaCl buffer (pH 7.8) contained in 2 mm quartz capillary tubes were placed in the cavity. Ethylene glycol was used to prevent the formation of ice crystals in frozen solution. EPR spectra were collected at 183K for 10-mers and at 100K for TAR RNAs by 1–5 scans over a sweep width of 250G with a microwave power of 0.2 mW, modulation amplitude of 0.8G, time constant of 328 ms, and sweep time of 168 s. For the room temperature EPR, 50 μM of 20 μl of TAR RNAs in 5 mM TEA and 50 mM NaCl buffer with different metal ions were placed in 1 mm quartz capillary tubes. EPR spectra were obtained after averaging 10–20 scans with a power of 2 mW and sweep time of 84 s.

Molecular Modeling of Spin-Labeled RNAs

Molecular modeling was performed with the INSIGHT II program (Accelrys Inc.). All 10 base-paired RNA duplexes with canonical A-type structures were constructed in the Biopolymer module, and two spin label molecules were attached at the desired 2′ positions for each duplex. Assuming that the structures of the 10-mer duplexes are rigid, the total energy of the spin labels was minimized with a final convergence of 0.001 kcal/mole, and dynamics calculations for the two spin labels and their tethers were performed at 298K for total of 45 ps in the cff force field using the Discover 3 module in Insight II. The interspin distances (distances between two nitroxide nitrogen atoms of the spin labels) were measured from the trajectory files, and distributions of the distances were obtained (Figure 2C). TAR RNA structures were retrieved from NMR structures (Protein Data Bank ID code 1ANR, no divalent ions) and the X-ray crystal structure (Nucleic Acid Database ID code URX075, 50 mM $CaCl_2$). Similar energy minimization and molecular dynamics (20 ps) were performed to determine the positions of the spin labels, while either the whole RNA or helical regions alone were kept rigid. Since the nucleotides in the bulge region of the TAR RNA are flexible relative to the helical regions, two types of simulation were examined to see the effect of the flexibility of nucleotides on measuring distances. First, as for the 10-mer duplexes, the whole RNA was fixed and energy minimization and MD calculations were performed. In the second trial, only helical regions were fixed and U23, C24, and U25 including the spin label were allowed to move freely during simulations. The distances obtained from the divalent metal-free structure range from 5.1–13.8 Å (avg. 9.8 Å) for fixed RNA calculations and 6.3–12.9 Å (avg. 9.1 Å) for flexible bulge calculations (Table 3B). However, the calculation from the crystal structure that contains calcium and magnesium ions shows longer distances ranging from 11.3–17.0 Å (avg. 14.1 Å) for the fixed RNA calculation and 11.2–19.0 Å (avg. 15.5 Å) for the flexible bulge calculations. In both cases, flexible motions of bulge nucleotides do not seem to affect the distance predictions significantly over our 20 ps time scale. Compared to the free motion of spin label in the duplexes, one important feature for TAR RNA during MD calculation is that the spin label at U25 was trapped in between C24 and G26, and the orientation of the spin label is limited to only one direction in both NMR and crystal structure simulations (Figure 3A).

Room Temperature TAR RNA EPR

EPR experiments at room temperature were repeated to examine the mobility of the spin labels at U25 and U40 of the TAR RNA and showed similar results as described in Edwards and Sigurdsson's work [11]. In the presence of 4.5 mM Mg^{2+} or 50 mM Ca^{2+} and 2.5 mM Mg^{2+} at pH 7.8, slight increases in spectral line width for TAR-divalent metal complexes were observed (data not shown), probably due to the formation of coaxially stacked stable structures.

Fourier Deconvolution Analysis of Interspin Distances

A method to analyze interspin distances from CW EPR line shapes using Fourier deconvolution has been described by Shin et al. [1, 13]. All calculations were performed using a MatLab v 6.5 (Math Works Inc.) as described [13]. Briefly, the EPR spectrum of two interacting spin labels, Π(B), can be interpreted as a convolution of the noninteracting absorption spectrum S(B) with a dipolar broadening function M(B) (Pake pattern). Following Fourier transformation of the experimental spectra, M(B) can be obtained from Equation 1:

$$M^*(\omega) = \Pi^*(\omega)/S^*(\omega), \quad (1)$$

where the function with superscript * represents the Fourier transformed function, and ω stands for the inverse variable of B. Since the experimental data obtained after Equation 1 contain noise at high frequencies, the data are truncated at 50ω. The data are then fit to a Gaussian function (Equation 2), and the inverse Fourier transform of that Gaussian is taken as the broadening function M(B) in Equations 3 and 4:

$$y = A \exp[-(1/\sigma)^2] + B, \quad (2)$$

$$\langle 2B \rangle = \int_{-\infty}^{\infty} |2B| \cdot M(B) dB / \int_{-\infty}^{\infty} M(B) dB, \quad (3)$$

$$\langle R \rangle = (0.75(3/2) g_e \beta_e / \langle 2B \rangle)^{\frac{1}{3}}. \quad (4)$$

Interspin distances are calculated from Equations 3 and 4, where $\langle 2B \rangle$ is the average splitting over the dipolar broadening function, g_e is the isotropic electron spin g value, β_e is the electron Bohr magneton, and $\langle R \rangle$ is the averaged spin-spin distance.

The experimental dipolar broadening function was fitted to the Gaussian function (Equation 2) defined above using a standard minimization search process (Nelder-Mead simplex search) with randomly chosen initial A, σ, and B values. In most of the cases, one Gaussian is sufficient to fit the broadening function. A sum of two Gaussian functions is taken when the single Gaussian fit is not

satisfactory. The correlation coefficient between the dipolar broadening function and the Gaussian fitting function is calculated as the sum of squared differences [$\Sigma (y_{bf} - y_{gf})^2$, where y_{bf} is the dipolar broadening function and y_{gf} is the Gaussian fitting function]. As an estimate of fitting errors, the value of σ in Equation 2 was allowed to vary such that the deviation of Gaussian fitting function from the dipolar broadening function was within $\pm$10% of the lowest value. This range of obtained distances is shown as error bars in Figure 4.

Acknowledgments

The authors thank Professor Y.-K. Shin (Iowa State University, Ames, IA) for assistance with Fourier deconvolution methods and Ann Hwang (Texas A&M University, College Station, TX) for early work on this project. This work was supported by the NIH (GM58096), the Robert A. Welch Foundation (A-1314), and the THECB Advanced Research Program. EPR facilities at Texas A&M are supported by the NSF (CHE-0092010).

Received: August 15, 2003
Revised: March 29, 2004
Accepted: April 21, 2004
Published: July 23, 2004

References

1. Berliner, L.J., Eaton, S.S., and Eaton, G.R. (2000). Biological Magnetic Resonance, Volume 19, Distance Measurements in Biological Systems by EPR (New York: Kluwer Academic/Plenum Publishers).
2. Hubbell, W.L., Cafiso, D.S., and Altenbach, C. (2000). Identifying conformational changes with site-directed spin labeling. Nat. Struct. Biol. *7*, 735–739.
3. Borbat, P.P., Mchaourab, H.S., and Freed, J.H. (2002). Protein structure determination using long-distance constraints from double-quantum coherence ESR: Study of T4 lysozyme. J. Am. Chem. Soc. *124*, 5304–5314.
4. Steinhoff, H.-J., and Suess, B. (2003). Molecular mechanisms of gene regulation studied by site-directed spin labeling. Methods *29*, 188–195.
5. Zhou, Y., Bowler, B.E., Lynch, K., Eaton, S.S., and Eaton, G.R. (2000). Interspin distances in spin-labeled metmyoglobin variants determined by saturation recovery EPR. Biophys. J. *79*, 1039–1052.
6. Keyes, R.S., Cao, Y.Y., Bobst, E.V., Rosenberg, J.M., and Bobst, A.M. (1996). Spin-labeled nucletide mobility in the boundary of the EcoRI endonuclease binding site. J. Biomol. Struct. Dyn. *14*, 163–172.
7. Qin, P.Z., Hideg, K., Feigon, J., and Hubbell, W.L. (2003). Monitoring RNA base structure and dynamics using site-directed spin labeling. Biochemistry *42*, 6772–6783.
8. Okonogi, T.M., Reese, A.W., Alley, S.C., Hopkins, P.B., and Robinson, B.H. (1999). Flexibility of duplex DNA on the submicrosecond timescale. Biophys. J. *77*, 3256–3276.
9. Macosko, J.C., Pio, M.S., Tinoco, I., Jr., and Shin, Y.-K. (1999). A novel 5′ displacement spin-labeling technique for electron paramagnetic resonance spectroscopy of RNA. RNA *5*, 1158–1166.
10. Qin, P.Z., Butcher, S.E., Feigon, J., and Hubbell, W.L. (2001). Quantitative analysis of the Isolated GAAA tetraloop/receptor interaction in solution: A site-directed spin labeling study. Biochemistry *40*, 6929–6936.
11. Edwards, T.E., Okonogi, T.M., and Sigurdsson, S.Th. (2002). Investigation of RNA-protein and RNA-metal ion interactions by electron paramagenetic resonance spectroscopy: The HIV TAR-Tat Motif. Chem. Biol. *9*, 699–706.
12. Edwards, T.E., Okonogi, T.M., Robinson, B.H., and Sigurdsson, S.Th. (2001). Site-specific incorporation of nitroxide spin-labels into internal sites of the TAR RNA; Structure-dependent dynamics of RNA by EPR spectroscopy. J. Am. Chem. Soc. *123*, 1527–1528.
13. Rabenstein, M.D., and Shin, Y.-K. (1995). Determination of the distance between two spin labels attached to a macromolecule. Proc. Natl. Acad. Sci. USA *92*, 8239–8243.
14. Persson, M., Harbridge, J.R., Hammarström, P., Mitri, R., Mårtensson, L.-G., Carlsson, U., Eaton, G.R., and Eaton, S.S. (2001). Comparison of electron paramagnetic resonance methods to determine distances between spin labels on human carbonic anhydrase II. Biophys. J. *80*, 2886–2897.
15. Gopalan, V., Kuhne, H., Biswas, R., Li, H., Brudvig, G.W., and Altman, S. (1999). Mapping RNA-protein interactions in ribonuclease P from Escherichia coli using electron paramagnetic resonance spectroscopy. Biochemistry *38*, 1705–1714.
16. Schiemann, O., Weber, A., Edwards, T.E., Prisner, T.F., and Sigurdsson, S.T. (2003). Nanometer distance measurements on RNA using PELDOR. J. Am. Chem. Soc. *125*, 3434–3435.
17. Pyle, A.M. (2002). Metal ions in the structure and function of RNA. J. Biol. Inorg. Chem. *7*, 679–690.
18. Bassi, G.S., Mollegaard, N.E., Murchie, A.I.H., and Lilley, D.M.J. (1999). RNA folding and misfolding of the hammerhead ribozyme. Biochemistry *38*, 3345–3354.
19. Zhuang, X., Kim, H., Pereira, M.J.B., Babcock, H.P., Walter, N.G., and Chu, S. (2002). Correlating structural dynamics and function in single ribozyme molecules. Science *296*, 1473–1476.
20. Tan, E., Wilson, T.J., Nahas, M.K., Clegg, R.M., Lilley, D.M.J., and Ha, T. (2003). A four-way junction accelerates hairpin ribozyme folding via a discrete intermediate. Proc. Natl. Acad. Sci. USA *100*, 9308–9313.
21. Walter, N.G., Harris, D.A., Pereira, M.J.B., and Rueda, D. (2002). In the fluorescent spotlight: Global and local conformational changes of small catalytic RNAs. Biopolymers *67*, 224–241.
22. Feng, S., and Holland, E.C. (1988). HIV-1 tat trans-activation requires the loop sequence within tar. Nature *334*, 165–167.
23. Jones, K.A., and Peterlin, B.M. (1994). Control of RNA initiation and elongation at the HIV-1 promoter. Annu. Rev. Biochem. *63*, 717–743.
24. Zacharias, M., and Hagerman, P.J. (1995). The bend in RNA created by the trans-activation response element bulge of human immunodeficiency virus is straightened by arginine and by Tat-derived peptide. Proc. Natl. Acad. Sci. USA *87*, 8985–8989.
25. Aboul-ela, F., Karn, J., and Varani, G. (1996). Structure of HIV-1 TAR RNA in the absence of ligands reveals a novel conformation of the trinucleotide bulge. Nucleic Acids Res. *24*, 3974–3981.
26. Ippolito, J., and Steitz, T. (1998). A 1.3-Å resolution crystal structure of the HIV-1 trans-activation response region RNA stem reveals a metal ion-dependent bulge conformation. Proc. Natl. Acad. Sci. USA *95*, 9819–9824.
27. Al-Hashimi, H.M., Pitt, S.W., Majumdar, A., Xu, W., and Patel, D.J. (2003). Mg^{2+}-induced variations in the conformation and dynamics of HIV-1 TAR RNA probed using NMR residual dipolar couplings. J. Mol. Biol. *329*, 867–873.
28. Nifosi, R., Reyes, C.M., and Kollman, P.A. (2000). Molecular dynamics studies of the HIV-1 TAR and its complex with argininamide. Nucleic Acids Res. *28*, 4944–4955.
29. Long, K.S., and Crothers, D.M. (1999). Characterization of the solution conformations of unbound and Tat peptide-bound forms of HIV-1 TAR RNA. Biochemistry *38*, 10059–10069.
30. Tiebel, B., Radzwill, N., Aung-Hilbrich, L.M., Helbl, V., Steinhoff, H.-J., and Hillen, W. (1999). Domain motions accompanying Tet repressor induction defined by changes of interspin distances at selectively labeled sites. J. Mol. Biol. *290*, 229–240.
31. Closs, G.L., Forbes, M.D.E., and Piotrowiak, P. (1992). Spin and reaction dynamics in flexible polymethylene biradicals as studied by EPR, NMR, and optical spectroscopy and magnetic field effect. Measurements and mechanisms of scalar electron spin-spin-coupling. J. Am. Chem. Soc. *114*, 3285–3294.
32. Silverman, S.K., and Cech, T.R. (1999). RNA tertiary folding monitored by fluorescence of covalently attached pyrene. Biochemistry *38*, 14224–14237.
33. Aurup, H., Tuschl, T., Benseler, F., Ludwig, J., and Eckstein, F. (1994). Oligonucleotide duplexes containing 2′-amino-2′-deoxycytidines: thermal stability and chemical reactivity. Nucleic Acids Res. *22*, 20–24.
34. Saenger, W. (1984). Principles of Nucleic Acid Structure (New York: Springer-Verlag), pp 51–101.

35. Fu, Z., Aronoff-Spencer, E., Backer, J.M., and Gerfen, G.J. (2003). The structure of the inter-SH2 domain of class IA phosphoinositide 3-kinase determined by site-directed spin labeling EPR and homology modeling. Proc. Natl. Acad. Sci. USA *100*, 3275–3280.
36. Altenbach, C., Oh, K.-J., Trabanino, R.J., Hideg, K., and Hubbell, W.L. (2001). Estimation of inter-residue distances in spin labeled proteins at physiological temperatures: experimental strategies and practical limitations. Biochemistry *40*, 15471–15482.
37. Bondensgaard, K., Mollova, E.T., and Pardi, A. (2002). The global conformation of the hammerhead ribozyme determined using residual dipolar couplings. Biochemistry *41*, 11532–11542.